Journal of Materials Chemistry C

Accepted Manuscript

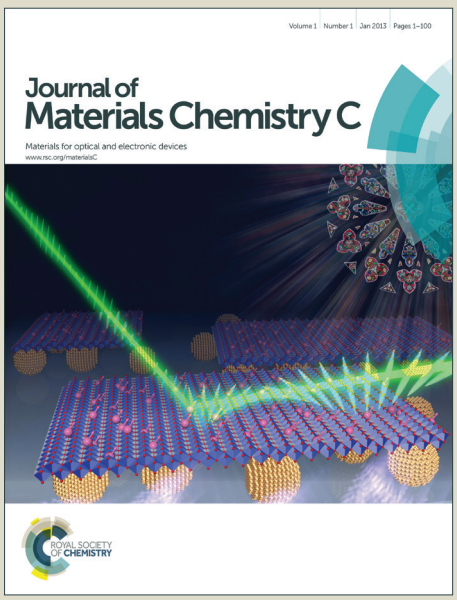

ROYAL SOCIETY OF CHEMISTRY

www.rsc.org/materialsC

Luminescence and electronic properties of $Ba_2MgSi_2O_7$: Eu^{2+}: A combined experimental and hybrid density functional theory study

Jing Yan,[a] Lixin Ning,*[,b] Yucheng Huang,[b] Chunmeng Liu,[a] Dejian Hou,[a]

Bingbing Zhang,[c] Yan Huang,[c] Ye Tao,[c] Hongbin Liang*[,a]

[a] *MOE Laboratory of Bioinorganic and Synthetic Chemistry, KLGHEI of Environment and Energy Chemistry, State Key Laboratory of Optoelectronic Materials and Technologies, School of Chemistry and Chemical Engineering, Sun Yat-sen University, Guangzhou 510275, China. E-mail: cesbin@mail.sysu.edu.cn*

[b] *Center for Nano Science and Technology, Department of Physics, Anhui Normal University, Wuhu, Anhui 241000, China. E-mail: ninglx@gmail.com*

[c] *Beijing Synchrotron Radiation Facility, Institute of High Energy Physics, Chinese Academy of Sciences, Beijing 100039, China*

Photoluminescence properties of $Ba_2MgSi_2O_7$:Eu^{2+} synthesized by a solid-state reaction method are first investigated in the vacuum ultraviolet (VUV) to visible (vis) excitation energy range. The band gap of the host is found to be around 7.44 eV. The incorporation of Eu^{2+} leads to bright green luminescence with weak thermal quenching above room temperature. Cathodoluminescence (CL) properties under low-voltage excitations are then studied, and the results suggest a potential application of the compound in field emission displays (FEDs). Electronic properties of the compound are finally calculated with a hybrid density functional theory (DFT) method, and are discussed in association with observed luminescence properties.

1. Introduction

Silicates have been widely applied as host compounds in phosphors for lighting and displays due to their good chemical and thermal stabilities, strong absorption of light in the VUV and ultraviolet (UV) regions, and intense luminescence when doped with proper lanthanide ions.[1,2] Among these, the europium-doped alkaline silicate compounds, $M_2MgSi_2O_7:Eu^{2+}$ (M=Ca, Sr, Ba), have received continuous attention for their potential uses as white light-emitting diode (LED) and persistent luminescent phosphors.[3-11] Especially, the monoclinic compound $Ba_2MgSi_2O_7:Eu^{2+}$ ($BMSO:Eu^{2+}$) is of importance in view of its photoluminescence properties under UV excitation. It exhibits an intense luminescence band at around 500 nm, with weak thermal quenching above room temperature.[7-11] The host material crystallizes in a monoclinic structure with space group C2/c (No. 15).[12] The structure consists of two-dimensional layers of SiO_4 and MgO_4 tetrahedra connected to each other through common corners, perpendicular to the *b*-axis of the unit cell (Fig. 1a). The Ba^{2+} ions (site symmetry C_1) are located between the layers and are each coordinated by eight oxygen ions, with the average bond length of 2.813 Å.[12] The dopant Eu^{2+} ions are supposed to substitute into Ba^{2+} sites in view of the similar ionic radii of the two ions, and give rise to the green luminescence as a result of the electric dipole-allowed transition from the lowest level of the excited $4f^65d$ configuration to the $4f^7(^8S_{7/2})$ ground state.

In the present study, we extend previous studies of photoluminescence properties of $BMSO:Eu^{2+}$ by using VUV excitations with synchrotron radiation, and then investigate CL properties of the compound under low-voltage excitations. Furthermore, by using hybrid DFT calculations, electronic properties of the compound are discussed in association with its luminescence properties. The hybrid DFT methods have been shown to improve results on defect physics in wide band gap oxides,[13,14] when compared with the standard DFT methods,

due to the partial recovered discontinuity in the exchange correlation potential by mixing with the Hartree-Fock (HF) exchange. The paper is organized as follows. The experimental and computational methods are described in Section 2. The results of luminescence measurements and hybrid DFT calculations are presented and discussed in Section 3, with the final conclusions collected in Section 4.

2. Methodology

A series of polycrystalline samples, $Ba_{2-x}Eu_xMgSi_2O_7$ ($0.003 \leq x \leq 0.20$), was prepared by solid-state reaction at high temperature. The starting materials were analytical grade $BaCO_3$, MgO, SiO_2, and 99.99% purity Eu_2O_3. After being thoroughly mixed in an agate mortar, stoichiometric amounts of the materials were pre-fired in air at 800 ^oC for 2 h and then ground and sintered at 1270 ^oC for 5 h in a CO atmosphere. The phase purity and crystal structure of the synthesized samples were identified by X-ray diffraction (XRD) using a D8 ADVANCE diffractometer with Cu-Kα radiation at room temperature.

The vacuum ultraviolet excitation and corresponding emission spectra were measured at the VUV spectroscopy experimental station on beam line 4B8 of Beijing Synchrotron Radiation Facility (BSRF).[15] An Edinburgh FLS920 combined fluorescence lifetime and steady-state spectrometer was employed to measure the UV-vis excitation and corresponding emission spectra and the luminescence decay curves of the samples. The instrument is equipped with a CTI-Cryogenics temperature control system. A 450 W Xe900 lamp was used as the excitation source for the steady-state spectra, while for the luminescence decay curves, a 150 W F900 lamp with a pulse width of 1 ns and a pulse repetition rate of 40–100 kHz was employed as the excitation source. The fluorescence quantum yield was measured by a two port, 150 mm, $BaSO_4$ coated integrating sphere which fits directly into the FLS920 sample

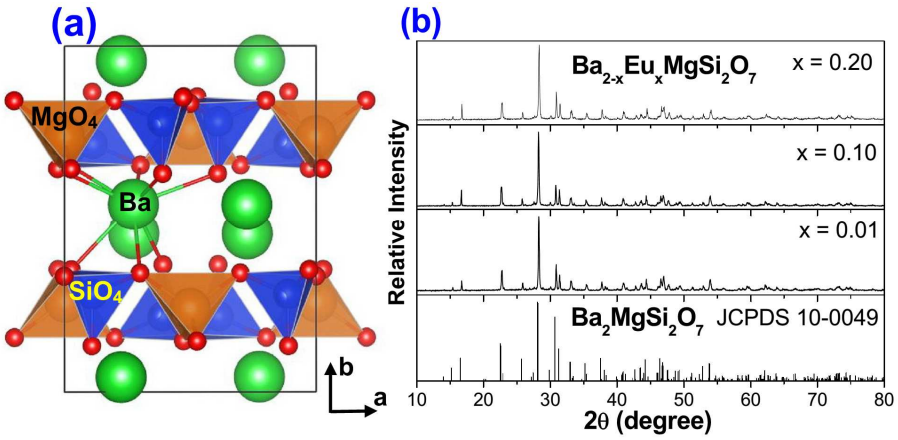

Fig. 1 (a) A schematic representation of the geometric structure of the BMSO unit cell. (b) The XRD patterns of the samples $Ba_{2-x}Eu_xMgSi_2O_7$ (x = 0.01, 0.10, 0.20) at room temperature along with the standard pattern (JCPDS 10-0049) of BMSO for comparison.

chamber. The internal quantum efficiency was evaluated as the ratio of the number of emission photons to that of absorption photons,[16] for which $BaSO_4$ was used as the standard sample to measure the number of photons not absorbed by the sample. The low-voltage CL measurements were performed in a vacuum chamber, where the phosphors are excited by an electron beam, and the emission spectra were recorded by a fiber spectrometer (Ocean Optics QEB0388) with a charge-coupled device camera.

In the DFT calculations, BMSO:Eu^{2+} was modeled by replacing one of 8 Ba atoms in the host unit cell with a Eu, corresponding to a chemical formula of $Ba_{2-x}Eu_xMgSi_2O_7$ with x = 0.25. The PBE0 hybrid functional[17] was used with the mixing parameter of HF exchange chosen to be α = 0.32, in order to match the calculated and experimental values of the host band gap. The Eu ($5s^25p^64f^76s^2$), Ba ($5s^25p^66s^2$), Mg ($2s^22p^63s^2$), Si ($3s^23p^2$) and O ($2s^22p^4$) were treated as valence electrons, and their interactions with the respective cores were described by the projected augmented wave (PAW) method.[18] In the excited-state calculations, a constrained approach was employed where one 4f electron of Eu^{2+} was promoted to the lowest-energy 5d state. The convergence criteria for total energies and atomic forces were set

to 10^{-6} eV and 0.01 eV $Å^{-1}$, respectively. The Monkhorst–Pack 3×3×3 k-mesh was used, and the cutoff energy of the plane wave basis was set to 550 eV. All the DFT calculations were carried out with the VASP package.[19,20]

3. Results and discussion

3.1. Photoluminescence properties

The XRD patterns of the selected samples $Ba_{2-x}Eu_xMgSi_2O_7$ (x=0.01, 0.10, 0.20) are displayed in Fig. 1b, and are compared with the standard pattern (JCPDS 10-0049) of the host. It is shown that the samples are of single phase structure, with no evident influence of the dopant Eu^{2+} on the crystal structure of the host. Fig. 2a plots the VUV-vis excitation spectra of $Ba_{1.9}Eu_{0.1}MgSi_2O_7$ at room temperature, when monitoring the Eu^{2+} 5d→ 4f emission at 501 nm. The excitation spectra exhibit two band maxima at 314 and 348 nm and a shoulder at 263 nm, which are attributed to a superposition of vibronic transitions from the $4f^7(^8S_{7/2})$ ground state to excited states of the $4f^65d^1$ configuration of Eu^{2+}. On the low energy side, the "staircase" structure characteristic of Eu^{2+} absorption is not resolved. Still, the position of the first transition, $4f^7$ $(^8S_{7/2}) \rightarrow 4f^6(^7F_0)5d_1$, can be roughly estimated to be at 438 ± 5 nm, where the transition intensity is 15–20% of that of the band maximum at 348 nm.[21] The band with maximum at 180 nm (6.89 eV) is ascribed to the host excitonic absorption, from which the host band gap is estimated to be ~1.08 × 6.89 = 7.44 eV, by taking into account the electron-hole binding energy in the excitonic state. This relationship between the excitonic absorption energy and the band gap was derived on the basis of compounds with known values of the two quantities.[22]

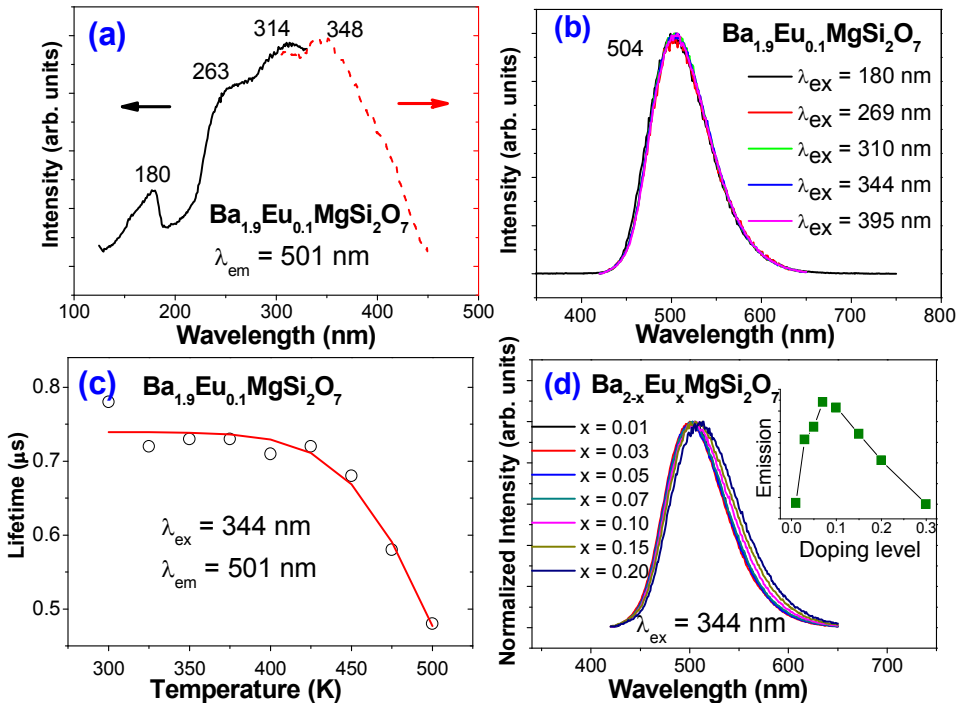

Fig. 2 (a) The VUV-vis excitation (λ_{em} = 501 nm) and (b) the normalized emission (λ_{ex} = 180, 269, 310, 344 and 395 nm) spectra of $Ba_{1.9}Eu_{0.1}MgSi_2O_7$ at room temperature. (c) The dependence of Eu^{2+} luminescence lifetime in $Ba_{1.9}Eu_{0.1}MgSi_2O_7$ on temperature between 300 and 500 K (λ_{ex} = 344 nm, λ_{em} = 501 nm), with the experimental data represented by full circles and the fitting curve by the solid line. (d) The normalized emission spectra (λ_{ex} = 344 nm) of $Ba_{2-x}Eu_xMgSi_2O_7$ with different Eu^{2+} concentrations (x = 0.01–0.20) at room temperature, with the inset curve showing the dependence of the emission intensity on the doping concentration.

Fig. 2b plots the normalized emission spectra of $Ba_{1.9}Eu_{0.1}MgSi_2O_7$ upon excitation at 180, 269, 310, 344 and 395 nm at room temperature. The spectra almost overlap with each other with a maximum at ~504 nm. This indicates that the emission bands originate from the Eu^{2+} centers of the same type, which are located on Ba^{2+} sites due to the small difference between their ionic radii (1.25 Å versus 1.42 Å).[23] The Stokes shift, which is defined as the energy difference between the maximum of the emission band and that of the lowest-energy absorption band (~436 nm), is around 2990 ± 105 cm^{-1}, in line with those observed for Eu^{2+}

emission in other silicates.[24] The bright green luminescence has a CIE chromaticity coordinate of x = 0.280 and y = 0.492, and the internal quantum efficiency of the phosphor was determined to be ~72% under 344 nm excitation.

The dependence of Eu^{2+} luminescence lifetime on temperature in $Ba_{1.9}Eu_{0.1}MgSi_2O_7$ is schematically presented in Fig. 2c. The lifetime was measured to be ~0.78 μs at room temperature, and starts to decrease at around 425 K due to thermal quenching. This behavior may be described by the equation,

$$\tau = \frac{\tau_0}{1 + \tau_0 \Gamma_0 \exp(-E_a / kT)}$$

where E_a is an activation energy for thermal quenching, τ_0 is the radiative lifetime, Γ_0 is the attempt rate, and k is the Boltzmann constant. A least-square fitting of the formula to the experimental data (Fig. 2c) yields E_a = 0.64 eV, $\Gamma_0 = 2.15\times10^{12}$ Hz and τ_0 = 0.74 μs. With the known value of E_a, the thermal quenching temperature $T_{0.5}$ was estimated to be ~435 K, based on the crude relationship between E_a and $T_{0.5}$, i.e., $E_a = T_{0.5}/680$ eV.[25] The value of E_a is consistent with those reported earlier,[6,10] and is larger than those determined for other Eu^{2+}-doped silicates, for example, $Cs_2MgSi_5O_{12}$ (0.196 eV),[26] $BaMgSi_4O_{10}$ (0.21 eV),[27] $Ba_2CaMg_2Si_6O_{17}$ (0.22 eV),[28] $CsAlSi_2O_6$ (0.27 eV),[29] $Na_2Ba_2Si_2O_7$ (0.34 eV),[30] $Sr_2MgSi_2O_7$ (0.40 eV),[31] and $Li_2Ca_2Si_2O_7$ (0.51 eV).[32] The activation energy E_a is supposed to be the energy required to promote an electron from the lowest vibrational level of the first $4f^6 5d_1$ excited state to the bottom of the host conduction band (CB). This comparison illustrates good thermal stability of Eu^{2+} luminescence in $Ba_{1.9}Eu_{0.1}MgSi_2O_7$.

The normalized emission spectra of $Ba_{2-x}Eu_xMgSi_2O_7$ with different doping levels (x = 0.01–0.20) are displayed in Fig. 2d, under 344 nm excitation at room temperature. The figure shows that the emission maximum shifts slightly to longer wavelengths by up to 10 nm with increasing Eu^{2+} concentration, which can be attributed to the effect of enhanced self-absorption at higher doping levels. The inset of Fig. 2d depicts the dependence of the

integrated Eu^{2+} emission intensity upon the doping level in the range x = 0.01–0.20. One can see that the luminescence intensity increases initially with Eu^{2+}concentration, maximizing at x = 0.07 and then decreasing gradually due to concentration quenching.

3.2. Low-voltage CL properties

In view of the bright green luminescence and good thermal stability, luminescence properties of $Ba_{1.9}Eu_{0.1}MgSi_2O_7$ under low-voltage cathode ray excitations were investigated. The CL spectrum of the phosphor under excitation of 30 $\mu A \cdot cm^{-2}$ and 2 kV is displayed in Fig. 3a, together with that of the commercial green phosphor Zn_2SiO_4: Mn^{2+} (ZSM)[33] for comparison. The inset of the figure shows the corresponding luminescence photographs. We observe that the peak wavelength and intensity of the emission band of $Ba_{1.9}Eu_{0.1}MgSi_2O_7$ are shorter (by 14 nm) and lower than those of ZSM, respectively. Nevertheless, the emission band of $Ba_{1.9}Eu_{0.1}MgSi_2O_7$ is broader than that of ZSM, resulting from the fact that the Eu^{2+} d-f transition is parity-allowed whereas the Mn^{2+} d-d transition is parity-forbidden. The integrated CL intensity of the former compound was evaluated to be about 111% of that of the latter, highlighting the intense emission of $Ba_{1.9}Eu_{0.1}MgSi_2O_7$ under low-voltage electron beam excitations.

The dependences of the CL emission intensity of $Ba_{1.9}Eu_{0.1}MgSi_2O_7$ on the accelerating voltage and the current density are displayed in Figs. 3b and 3c, respectively. It shows that, with the current density fixed at 30 $\mu A \cdot cm^{-2}$, the CL intensity increases with the increasing accelerating voltage, which is attributed to the larger penetration depth produced by the higher electron beam current intensity (Fig. 3b). When the accelerating voltage is fixed at 2 kV, the CL intensity increases with the increase of the current density, without saturation up to 130 $\mu A \cdot cm^{-2}$ (Fig. 3c). These CL properties together with those observed in photoluminescence measurements suggest a potential application of $Ba_{1.9}Eu_{0.1}MgSi_2O_7$ in FEDs.

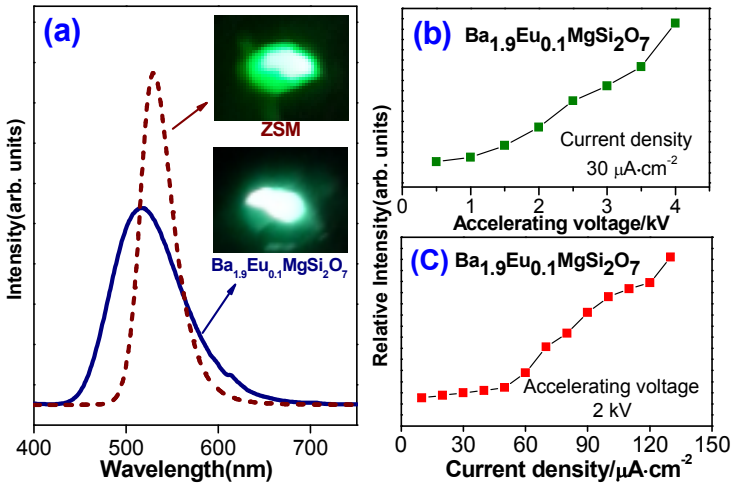

Fig. 3 (a) CL spectra of $Ba_{1.9}Eu_{0.1}MgSi_2O_7$ and commercial ZSM under cathode ray excitation (excitation voltage = 2 kV, current density = 30 μA·cm^{-2}). The inset shows the luminescence photographs of the two phosphors. The CL intensities of the sample as a function of accelerating voltage (b) and current density of electron beam (c) are also shown.

3.3. Hybrid DFT calculations

The calculated lattice parameters for pure BMSO with the DFT-PBE0 method agree very well with experimental values,[20] with the deviations no larger than 0.5%. For the model system $Ba_{1.75}Eu_{0.25}MgSi_2O_7$, the substitution of Eu^{2+} for a Ba^{2+} induces a slight decrease of the unit cell volume (by –1.119%), and distorts the monoclinic phase of the undoped system into a triclinic one with the deviations of angles within ±0.135°. The distances from the dopant site to the coordinated oxygens are also decreased upon the Eu_{Ba} substitution, in the range of 0.014–0.153 Å. This is consistent with the smaller ionic radius of Eu^{2+} than that of Ba^{2+} by 0.18 Å in the eightfold coordination.

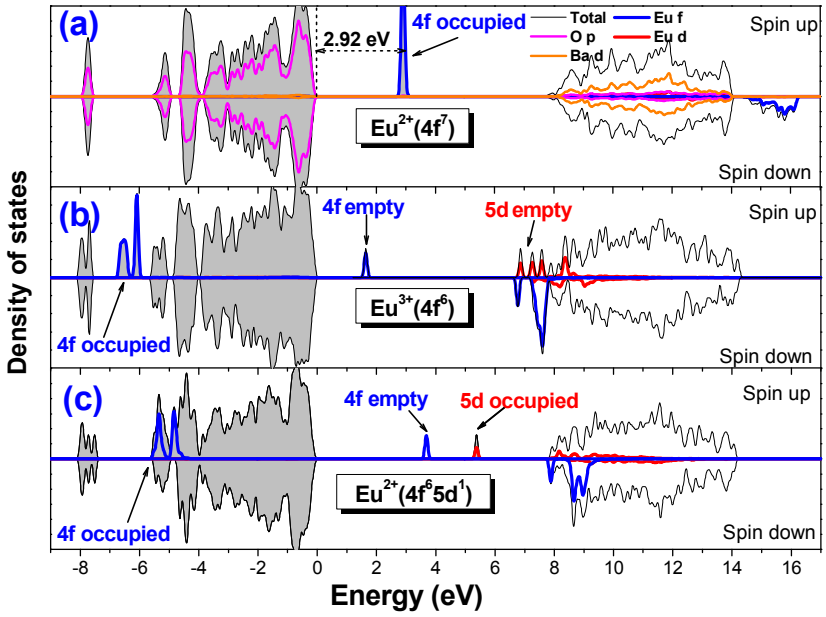

Fig. 4 Calculated total and orbital-projected DOS for the $Ba_2MgSi_2O_7$ crystals doped with $Eu^{2+}(4f^7)$ (a), $Eu^{3+}(4f^6)$ (b), and $Eu^{2+}(4f^65d_1)$ (c). The top of the O 2p valence band is set at zero energy.

Fig. 4a shows the total and orbital-projected densities of states (DOSs) for $Ba_{1.75}Eu_{0.25}MgSi_2O_7$ in the $4f^7$ ground state of Eu^{2+}. The top of the host valence band (VB) is dominated by O 2p states, and the bottom of the host CB is mainly formed by Ba 5d states with a small contribution from O 2p states through Ba–O bonding. The CB edge is represented by a small peak at 7.48 eV above the top of O 2p VB, composed mainly of the s-character states of Ba and O atoms. The relatively large dispersion of the O 2p states (~8.0 eV) originates from the existence of four symmetrically distinct oxygens in $Ba_2MgSi_2O_7$. The top (at 0 eV) of the O 2p band is contributed by the oxygens each bonded to a single Si atom, whereas the bottom (at –8.0 eV) is derived from those each saturated with two Si-O bonds. Moreover, the incorporation of the ground-state Eu^{2+} in $Ba_2MgSi_2O_7$ leads to the formation of seven occupied 4f states inside the host band gap, which is by ~2.92 eV above the top of the

O 2p VB, along with a large exchange splitting. The Eu^{2+} 5d states are resonant with the CB, hybridizing with Ba 5d and O 2p states.

The CL process involves the impact of a high energy electron beam on the phosphor, which can promote electrons into the CB and leave behind holes in the VB of the host. The ground-state Eu^{2+} ($4f^7$) may capture a hole from the VB to become Eu^{3+} ($4f^6$). The DOSs for such Eu^{3+}-doped BMSO are displayed in Fig. 4b. It shows that the six occupied 4f states in Eu^{3+} ($4f^6$) are located deeply inside the VB, with the remaining empty 4f state still within the band gap. More interestingly, three empty 5d states are now positioned below the CB edge, in contrast with the case of Eu^{2+} ($4f^7$) (Fig. 4a). The lowest $5d_1$ state is thus able to trap an electron from the CB to become the excited-state $Eu^{2+}(4f^65d_1)$ from which the 5d→4f emission occurs. The DOSs for this excited state are plotted in Fig. 4c, which shows that the $5d_1$ state will shift further inside the band gap when it is occupied by an electron. Therefore, the above results show that the positions of Eu^{2+}/Eu^{3+} 4f and 5d states relative to the host VB or CB depend strongly on the electron occupation. This reflects the large Coulomb interaction among the 4f and 5d electrons and the screening effect of the 4f electrons on the 5d states. Furthermore, we see that, in the CL process of Eu-doped $Ba_2MgSi_2O_7$, Eu^{2+} must first capture a hole from the VB to form an empty electron-trapping $5d_1$ state, before it can trap an electron from the CB to produce the emitting $4f^65d_1$ excited state.

4. Conclusions

In summary, luminescence and electronic properties of Eu^{2+}-doped BMSO compound have been investigated experimentally and theoretically. Under photoexcitation in the VUV-vis region, the compound exhibits bright green luminescence centered around 504 nm with a high thermal quenching temperature, resulting from the 5d→4f transition of Eu^{2+} with the emitting

level well below the host CB edge. Low-voltage CL measurements of the compound were then conducted, and the comparison of the results with those of the commercial green phosphor ZSM suggests a potential application of BMSO:Eu^{2+} in FEDs. With the help of hybrid DFT calculations, electronic properties of the ground-state $Eu^{2+}(4f^7)$ and $Eu^{3+}(4f^6)$ and the excited-state $Eu^{2+}(4f^6 5d_1)$ in BMSO have been examined. It was found that, although the $5d_1$ state is located within the host CB in $Eu^{2+}(4f^7)$, it moves below the CB edge in $Eu^{2+}(4f^6 5d_1)$ and $Eu^{3+}(4f^6)$, consistent with the observation of efficient Eu^{2+} 5d→4f luminescence under optical and low-voltage electron beam excitations. The present work also demonstrates the usefulness of hybrid DFT calculations to enhance our understanding of luminescence and electronic properties of Eu^{2+} centers in ionic compounds, which have a wide application in the field of optical materials.

Acknowledgements

The work is financially supported by National Natural Science Foundation of China (Nos. 10979027, 11174005, 21171176 and U1232108), Guangzhou Science and Technology Project (2013Y2-00118) and Natural Science Foundation of Guangdong Province (S2013030012842).

Notes and references

1 G. Blasse, B. C. Grabmaier, *Luminescent Materials*, Springer, Berlin, 1994.

2 W. M. Yen, A. Shionoya, H.Yamamoto, *Phosphor Handbook*, CRC Press, Boca Raton, FL, 2007.

3 H. Lin, C. W. Nan, X. S. Zhou, J. B. Wu, H. F. Wang, D. P. Chen, and S. M. Xu, *Mater. Chem. Phys.* 2003, **82**, 860.

4 D. W. He, Y. N. Shi, D. Zhou, and T. Hou, *J. Lumin.*, 2007, **122–123**, 158.

5 T. Kim, Y. Kim, S. Kang, *Appl. Phys. B*, 2012, **106**, 1009.

6 G. Blasse, W. L. Wanmaker, and J. W. Tervugt, *J. Electrochem. Soc.*, 1968, **115**, 673.

7 T. Aitasalo, D. Hreniak, J. Holsa, T. Laamanen, M. Lastusaari, J. Niittykoski, F. Pelle, and W. Strek, *J. Lumin.*, 2007, **122–123**, 110.

8 S. Yao, Y. Li, L. Xue, and Y. Yan, *J. Am. Ceram. Soc.*, 2010, **93**, 3793.

9 X. Zhang, J. Zhang, R. Wang, and M. Gong, *J. Am. Ceram. Soc.*, 2010, **93**, 1368.

10 H. Wu, Y. Hu, B. Zeng, Z. Mou, L. Deng, *J. Phys. Chem. Solids*, 2011, **72**, 1284.

11 T. H. Tam, N. V. Du, N. D. T. Kien, C. X. Thang, N. D. Cuong, P. T. Huy, N. D. Chien, D. H. Nguyen, *J. Lumin.*, 2014, **147**, 358.

12 T. Aitasalo, J. Hölsä, T. Laamanen, M. Lastusaari, L. Lehto, J. Niittykoski, and F. Pellé, *Z. Kristallogr. (Suppl.)*, 2006, **23**, 481.

13 F. Oba, A. Togo, I. Tanaka, J. Paier, G. Kresse, *Phys. Rev. B*, 2008, **77**, 245202.

14 A. Janotti, J. B. Varley, P. Rinke, N. Umezawa, G. Kresse, C. G. Van de Walle, *Phys. Rev. B*, 2010, **81**, 085212.

15 Y. Tao, Y. Huang, Z. Gao, H. Zhuang, Z. Guo, H. Zhuang, A. Zhou, Y. Tan, D. Li, S. Sun, *J. Synchrotron Radiat.*, 2009, **16**, 857.

16 Y. Xu, X. Zhang, S. Dai, B. Fan, H. Ma, J. Adam, J. Ren, G. Chen, *J. Phys. Chem. C*, 2011, **115**, 13056.

17 J. P. Perdew, M. Ernzerhof, K. Burke, *J. Chem. Phys.*, 1996, **105**, 9982.

18 P. E. Blöchl, *Phys. Rev. B*, 1994, **50**, 17953.

19 G. Kresse, J. Furthmüller, *Phys. Rev. B*, 1996, **54**, 11169.

20 G. Kresse, D. Joubert, *Phys. Rev. B*, 1999, **59**, 1758.

21 P. Dorenbos, *J. Phys.: Condens. Matter*, 2003, **15**, 575.

22 P. Dorenbos, *J. Lumin.*, 2005, **111**, 89.

23 R. D. Shannon, *Acta Crystallogr. A*, 1976, **32**, 751.

24 P. Dorenbos, *J. Lumin.*, 2003, **104**, 239.

25 P. Dorenbos, *J. Phys.: Condens. Matter*, 2005, **17**, 8103.

26 D. Wei, F. Du, Y. Huang, H. J. Seo, *Materials Letters*, 2011, **65**, 2711.

27 B. Yuan, Y. Huang, Y. M. Yu, S. I. Kim, H. J. Seo, *Materials Letters*, 2012, **70**, 57.

28 B. Yuan, Y. Huang, Y. M. Yu, H. J. Seo, *Ceramics International*, 2012, **38**, 2219.

29 W. Zhang, D. Wei, H. J. Seo, *Materials Letters*, 2013, **94**, 140.

30 J. Sun, D. Cui, H. Du, *Appl. Phys. B*, 2013, **111**, 537.

31 X. Zhang, X. Tang, J. Zhang, H. Wang, J. Shi, M. Gong, *Powder Technology*, 2010, **204**, 263.

32 J. S. Kim, H. J. Song, H. S. Roh, D. K. Yim, J. H. Noh, K. S. Hong, *Materials Letters,* 2012, **79**, 112.

33 P. H. Holloway, T. A. Trottier, B. Abrams, C. Kondoleon, S. L. Jones, J. S. Sebastian, and W. J. Thomes, *J. Vac. Sci. Technol. B,* 1999, **17**, 758.

TOC entry

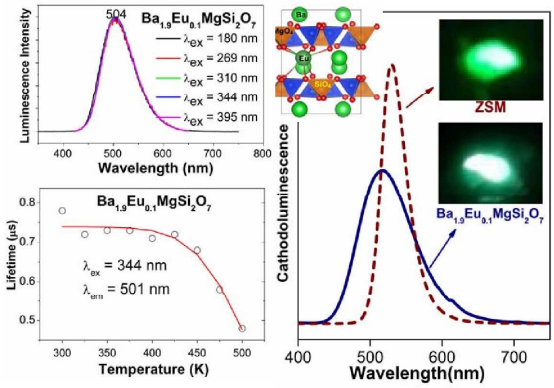

Luminescence and electronic properties of $Ba_2MgSi_2O_7:Eu^{2+}$ were investigated under optical and low-voltage cathode ray excitations and by hybrid DFT calculations.